Interacting Particle System based estimation of reach probability of General Stochastic Hybrid Systems

Ma, Hao; Blom, Henk A.P.

DOI
10.1016/j.nahs.2022.101303

Publication date
2023

Document Version
Final published version

Published in
Nonlinear Analysis: Hybrid Systems

Nonlinear Analysis: Hybrid Systems 47 (2023) 101303

Contents lists available at ScienceDirect

Nonlinear Analysis: Hybrid Systems

journal homepage: www.elsevier.com/locate/nahs

Interacting Particle System based estimation of reach probability of General Stochastic Hybrid Systems

Hao Ma [a,b,*], Henk A.P. Blom [a]

[a] Delft University of Technology, 2629 HS Delft, The Netherlands
[b] Civil Aviation College, Northwestern Polytechnical University, 710072 Xi'an, China

ARTICLE INFO

Article history:
Received 10 September 2021
Received in revised form 22 May 2022
Accepted 22 October 2022
Available online xxxx

Keywords:
Interacting Particles
Factorization
Rare event
Reach probability
Stochastic Hybrid System

ABSTRACT

For diffusions, a well-developed approach in rare event estimation is to introduce a suitable factorization of the reach probability and then to estimate these factors through simulation of an Interacting Particle System (IPS). This paper studies IPS based reach probability estimation for General Stochastic Hybrid Systems (GSHS). The continuous-time executions of a GSHS evolve in a hybrid state space under influence of combinations of diffusions, spontaneous jumps and forced jumps. In applying IPS to a GSHS, simulation of the GSHS execution plays a central role. From literature, two basic approaches in simulating GSHS execution are known. One approach is direct simulation of a GSHS execution. An alternative is to first transform the spontaneous jumps of a GSHS to forced transitions, and then to simulate executions of this transformed version. This paper will show that the latter transformation yields an extra Markov state component that should be treated as being unobservable for the IPS process. To formally make this state component unobservable for IPS, this paper also develops an enriched GSHS transformation prior to transforming spontaneous jumps to forced jumps. The expected improvements in IPS reach probability estimation are also illustrated through simulation results for a simple GSHS example.

1. Introduction

A Stochastic Hybrid System (SHS) as defined by Hu et al. [1] involves two dynamically interacting state components, i.e. a discrete-valued θ_t and a continuous-valued x_t. The θ_t component may switch when x_t hits a θ_t-dependent boundary. The x_t component evolves under influence of θ_t-dependent Brownian motion and forced jumps at moments of hitting a θ_t-dependent boundary. Bujorianu and Lygeros [2] define a General SHS (GSHS) by extending an SHS with spontaneous jumps, the rate λ of which depends on the joint state (x_t, θ_t). Well-known sub-classes of GSHS executions are solutions of SDE's driven by Brownian motion and spontaneous jumps generated by Poisson random measure. Specific subclasses are Markov switching diffusions [3], hybrid switching diffusions [4] and hybrid switching jump-diffusions [5]. These developments include methods for the numerical integration of both spontaneous jumps and Brownian motion. Teel et al. [6] provide an in-depth survey regarding stability analysis of GSHS and various sub-classes.

A GSHS can be transformed to an SHS of Hu et al. [1] by capturing each spontaneous jump as a forced jump at an exit time condition [7]. More specifically, an auxiliary state component q_t, representing "remaining local time", starts at each exit time as an exponentially distributed random variable, subsequently evolves as $dq_t = -\lambda(\theta_t, x_t)dt$, and defines

* Corresponding author at: Delft University of Technology, 2629 HS Delft, The Netherlands.
E-mail addresses: h.ma-2@tudelft.nl (H. Ma), h.a.p.blom@tudelft.nl (H.A.P. Blom).

https://doi.org/10.1016/j.nahs.2022.101303

a new exit time upon reaching value zero. As shown in the stochastic hybrid systems survey by Lygeros and Prandini [7], the mainstream of stochastic hybrid control developments address diffusion and forced jumps only; e.g. [8,9]. A key exception is optimal control of a Markov switching diffusion via its SDE coefficients and spontaneous jump rate [10].

As will be shown in this paper, there may be unexpected effects when transforming spontaneous jumps in a GSHS to forced jumps in an SHS. This paper studies the role played by these unexpected effects in estimating stochastic reach probability for a GSHS using the Interacting Particle System (IPS) approach of Cérou et al. [11]. The objective is to learn understanding the effect on IPS of transforming spontaneous jumps to forced jumps.

Bujorianu [12] provides an in-depth overview of stochastic reachability analysis for hybrid systems, including GSHS. Stochastic reach probability estimation is a safety verification problem (e.g. [13–15]) that has been well studied in the control systems domain and in the safety domain. In the control domain the focus is on developing an (approximate) abstraction of the system for which it can be shown that the reach probability problem is sufficiently similar [16,17]. Approximate abstractions typically make use of a finite partition of the state space (e.g. [13,18,19]).

In the safety domain, reach probability is evaluated using a finite partition method or statistical simulation. For realistic applications, the latter requires support from analytical methods to reduce variance. Literature on such variance reduction distinguishes two main approaches: importance sampling (IS) and multi-level importance splitting (ISp). IS draws samples from a reference stochastic system model in combination with analytical compensation for sampling from the reference model instead of the intended model. Bucklew [20] gives an overview of IS and analytical compensation mechanisms. For complex models analytical compensation mechanisms typically fall short and multi-level ISp is the preferred approach (e.g. [21–24]).

The basic idea of multi-level ISp is to enclose the target set, i.e., the set for which the reach probability has to be estimated by a series of nested subsets. Each time a simulated particle hits one of the nested subsets, the particle may be split into multiple copies. This multi-level setting allows to express the small reach probability of the inner level set as a product of larger reach probabilities for the sequence of nested subsets (see, e.g., [25]). Cérou et al. [11,26] embedded this multi-level factorization in the Feynman–Kac factorization equation for strong Markov processes [27]. This Feynman–Kac setting subsequently supported the evaluation of the reach probability through sequential Monte Carlo simulation in the form of an Interacting Particle System (IPS), including proof of convergence [11]. Krystul et al. [28] have used the Feynman–Kac setting to prove convergence of IPS using sampling per mode for a switching diffusion.

Because the theoretical setting of IPS [11] includes strong Markov processes, and a GSHS execution is strong Markov [2], IPS theory applies to GSHS. Blom et al. [29,30] apply IPS to rare event estimation for an SHS model of an advanced air traffic scenario, which is obtained through applying a Lygeros and Prandini [7] type of transformation to the underlying GSHS. The hybrid state space of this SHS model is very large, i.e., 490 discrete states and a 28-dimensional Euclidean state space. To prevent particle depletion or impoverishment, a very large number of particles is used. In an attempt to improve the quality of the set of particles, Blom et al. [31,32] develop and apply a further IPS extension for an SHS with a large number of modes. Complementarily, Prandini et al. [33] investigate the integration of air traffic complexity model with IPS. For a true GSHS setting, Blom et al. [34] showed that the use of different numerical integration methods in applying IPS to a true GSHS may have unexpected effects on reach probability estimation. However, these studies did not lead to a basic understanding of the underlying mechanisms. This paper aims to close this gap in basic understanding.

This paper is organized as follows. Section 2 presents background of GSHS and the transformation to SHS. Section 3 reviews IPS theory and presents the algorithmic steps and particle splitting options for an arbitrary GSHS. Section 4 specifies three IPS-FAS algorithms for GSHS, two of which make use of the transformation to SHS of Hu et al. [1]. Section 5 illustrates results of IPS-FAS algorithms from Section 4 applied to a simple GSHS example. Section 6 draws conclusions.

2. General Stochastic Hybrid System (GSHS)

Throughout this and the following sections, all stochastic processes are defined on a complete stochastic basis $(\Omega, \mathcal{F}, \mathbb{F}, \mathrm{P}, \mathcal{T})$ with $(\Omega, \mathcal{F}, \mathrm{P})$ being a complete probability space and $\mathbb{F}$ an increasing sequence of sub-σ-algebras on the time line $\mathcal{T} = \mathbb{R}_+$, i.e., $\mathbb{F} \triangleq \{\mathcal{J}, (\mathcal{F}_t, t \in \mathbb{R}_+), \mathcal{F}\}$, with $\mathcal{J}$ containing all P-null sets of $\mathcal{F}$ and $\mathcal{J} \subset \mathcal{F}_s \subset \mathcal{F}_t \subset \mathcal{F}$ for every $s < t$.

2.1. GSHS definition

Bujorianu and Lygeros [2] formalized the concept of GSHS or general stochastic hybrid automata as follows:

Definition 1 (*GSHS*)**.** A GSHS is a collection $(\Theta, d, X, f, g, Init, \lambda, R)$ where

- Θ is a countable set of discrete-valued variables;
- $d: \Theta \to \mathbb{N}$ is a map giving the dimensions of the continuous state spaces;
- $X: \Theta \to \mathbb{R}^{d(\cdot)}$ maps each $\theta \in \Theta$ into an open subset X^θ of $\mathbb{R}^{d(\theta)}$;
- $f: \Xi \to \mathbb{R}^{d(\cdot)}$ is a vector field, where $\Xi \triangleq \bigcup_{\theta \in \Theta} \{\theta\} \times X^\theta$;
- $g: \Xi \to \mathbb{R}^{d(\cdot) \times m_{\mathrm{dim}}}$ is an $X^{(\cdot)}$-valued matrix, $m_{\mathrm{dim}} \in \mathbb{N}$;
- Init: $\beta(\Xi) \to [0, 1]$ an initial probability measure on Ξ;
- $\lambda: \overline{\Xi} \to \mathbb{R}^+$ is a transition rate function;
- $R: \overline{\Xi} \times \beta(\overline{\Xi}) \to [0, 1]$ is a transition measure.

2.2. GSHS execution

Definition 2 (*GSHS Execution*)**.** A stochastic process $\{\theta_t, x_t\}$ is called a solution of GSHS execution if there exists a sequence of stopping times $s_0 = 0 < s_1 < s_2 < \cdots$ such that:

- (θ_0, x_0) is a Ξ-valued random variable satisfying the probability measure *Init*;
- For $t \in \left[s_{j-1}, s_j\right), j \geq 1$, θ_t, x_t is a solution of the SDE:

$$\begin{aligned} d\theta_t &= 0 \\ dx_t &= f(\theta_t, x_t)dt + g(\theta_t, x_t)dW_t \end{aligned} \tag{1}$$

  with W_t m-dimensional standard Brownian motion;

- s_j is the minimum of the following two stopping times: (i) first hitting time $> s_{j-1}$ of the boundary of $X^{\theta_{s_{j-1}}}$ by the phase process $\{x_t\}$; and (ii) first moment $> s_{j-1}$ of a transition event to happen at rate $\lambda(\theta_t, x_t)$.
- At stopping time s_j the novel hybrid state $\{\theta_{s_j}, x_{s_j}\}$ satisfies the conditional probability measure $p_{\theta_{s_j}, x_{s_j}|\theta_{s_j-}, x_{s_j-}}(A|\theta, x) = R((\theta, x), A)$ for any $A \in \beta(\Xi)$.

In order to assure that a GSHS execution has a solution the following assumptions are adopted:

A1 (non-Zeno property): $E\{s_j - s_{j-1}\} > 0$, P-a.s.

A2: For each $(\theta_0, x_0) \in \Xi$, Eq. (1) has a pathwise unique solution on a finite time interval $[0, T]$.

A3 λ is measurable and finite valued.

A4 $Init(\Xi) = 1$, and $R((\theta, x), \Xi) = 1$ for each $(\theta, x) \in \overline{\Xi}$.

Bujorianu and Lygeros [2] show that the stochastic process $\{\theta_t, x_t\}$ generated by execution of a GSHS satisfies the strong Markov property.

2.3. Stochastic analysis background of GSHS execution

Complementary to the probabilistic characterizations of GSHS [2,12,35], various subclasses of GSHS have been studied as solutions of stochastic differential equations on a hybrid state space that are driven by Brownian motion and Poisson random measure. These studies derive conditions for the existence of pathwise unique solutions, continuity of solutions relative to initial condition (Feller property), and convergent numerical integration schemes.

The best known subclass is Markov switching diffusion [3]; which forms a GSHS subclass satisfying the following restrictions:

(i) There are no boundary hittings, i.e. $X^\theta = \mathbb{R}^{d(\theta)}$;

(ii) Transition measure R does not support jumps in $\{x_t\}$, i.e. $R(\theta, x; \Theta, dy) = 0$ if $x \cap dy = 0$; and

(iii) Transition rate function $\lambda(\theta, x)$ is $x-$ invariant.

By dropping the third restriction, we get the subclass of hybrid switching diffusions [4]. As is well addressed by Yin and Zhu [4], the dependency of the mode process $\{\theta_t\}$on the phase process $\{x_t\}$ asks for complementary derivations regarding existence of pathwise unique solutions and Feller property. Yin and Zhu [4] also show weak converge of an adapted Euler–Maruyama integration scheme to hybrid switching diffusions.

By dropping both restriction (ii) and (iii), the subclass of hybrid switching diffusions emerges. Pathwise unique solutions have been derived by Blom [36], Ghosh and Bagchi [37] and Xi et al. [38]. Feller property has been derived by Krystul et al. [39], Xi et al. [38], Kunwai and Zhu [5] and Blom [40]. Convergent numerical integration has been addressed by Krystul [41, chapter 4], including approximation of the first hitting time of a boundary. The final step is to also drop restriction (i). This allows the generation of instantaneous jumps upon hitting boundaries of X^θ; pathwise unique solutions have been addressed by Krystul et al. [42].

2.4. Probabilistic transformation to an SHS

As explained by Lygeros and Prandini [7] a GSHS can be transformed to an SHS of Hu et al. [1]. This transformation consists of the following four changes: (i) An auxiliary state component q_t, representing "remaining local time", starts at an applicable stopping time τ at initial condition $q_\tau \sim \exp(1)$, and subsequently evolves as $dq_t/dt = -\lambda(\theta_t, x_t)$; (ii) The exit boundary of X^θ is extended with an extra boundary of the form $q_{t-} = 0$; and (iii) Spontaneous probabilistic jumps in $\{x_t, \theta_t\}$ are replaced by forced probabilistic jumps at moment $q_{t-} = 0$; and (iv) Upon reaching the extended exit boundary at stopping time τ' the "remaining local time" is resampled, i.e. $q_{\tau'} \sim \exp(1)$.

Hence, transformation of GSHS $(\Theta, d, X, f, g, Init, \lambda, R)$ to SHS $(\Theta^*, d^*, X^*, f^*, g^*, Init^*, R^*)$ works as follows:

- $\Theta^* = \Theta$
- $d^* = d + 1$
- $X^* = X \times (0, \infty)$
- $f^*(\theta, x, .) = \begin{bmatrix} f(\theta, x) & -\lambda(\theta, x) \end{bmatrix}^T$

- $g^*(\theta, x, .) = \begin{bmatrix} g(\theta, x) & 0 \end{bmatrix}^T$
- $\text{Init}^* = \begin{bmatrix} \text{Init} & q_0 \end{bmatrix}^T$ with $q_0 \sim \exp(1)$;
- $R^*((\theta, x, .); A \times dq) = R((\theta, x); A) \times \mathrm{e}^{-q} dq$

Execution of this SHS yields the SHS execution process $\{\theta_t^*, x_t^*, q_t^*\}$, which is a strong Markov process relative to its underlying increasing sequence of sigma algebras $\sigma\{\theta_s^*, x_s^*, q_s^*; s \in [0, t]\}$, $t \in \mathcal{T}$.

It should be noticed that from a stochastic perspective the process $\{\theta_t^*, x_t^*\}$ differs from the process $\{\theta_t, x_t\}$. The key difference is that the sigma algebra $\sigma\{\theta_s^*, x_s^*, q_s^*; s \in [0, t]\}$ includes "remaining local time", which implies (partial) information about the next hitting time of the boundary 0 of $(0, \infty)$, while the sigma algebra $\sigma\{\theta_s, x_s; s \in [0, t]\} \subset \mathrm{F}_t$, i.e. it does not include any information about such future event. To avoid abusing the extra information, the "remaining local time" component $\{q_t^*\}$ should be treated as being unobservable for other processes that depend on the GSHS execution.

An illustrative example is $\{x_t^*\}$ being a diffusion, the coefficients of which are a function of a Markov chain $\{\theta_t\}$. Under the above transformation, the coefficients of the new diffusion process $\{x_t^*\}$ still are a function of the new mode switching process $\{\theta_t^*\}$. However, the original Markov chain $\{\theta_t\}$ is transformed to a hybrid process $\{\theta_t^*, q_t^*\}$. The process $\{\theta_t^*\}$ switches when the Euclidean-valued "remaining local time" process $\{q_t^*\}$ hits the boundary 0 of $(0, \infty)$, i.e. $\{q_t^*\}$ foretells the next jump time of $\{\theta_t^*, q_t^*\}$.

3. IPS based reach probability estimation

3.1. GSHS reach probability

The problem is to estimate the probability γ that $\{\theta_t, x_t\}$ reaches a closed subset $D \subset \Xi$ within finite period $[0, T]$, i.e.

$$\gamma = P(\tau < T) \tag{2}$$

with τ being the first hitting time of D by $\{\theta_t, x_t\}$:

$$\tau = \inf\{t > 0, (\theta_t, x_t) \in D\} \tag{3}$$

Remark. Cérou et al. [11] and L'Equyer et al. [22] also address the more general situation that T is a P-a.s. finite stopping time.

Cérou et al. [11] developed the IPS theory and algorithmic steps for estimating reach probability for a strong Markov process on a general Polish state space. Thanks to the strong Markov property of the process $\{\theta_t, x_t\}$ defined by the execution of the GSHS in Section 2, the IPS approach applies to the estimation of GSHS reach probability.

3.2. Multi-level factorization of reach probability

The principle in factorizing the reach probability $\gamma = P(\tau < T)$ is to introduce a sequence D_k, $k = 0, \ldots, m$, of nested closed subsets of Ξ, i.e. $D = D_m \subset D_{m-1} \subset \cdots \subset D_1 \subset D_0 = \Xi$, with D_1 such that $P\{(\theta_0, x_0) \in D_1\} = 0$. Let τ_k be the first moment in time that $\{\theta_t, x_t\}$ reaches D_k, i.e.

$$\tau_k = \inf\{t > 0;\ (\theta_t, x_t) \in D_k \vee t \geq T\} \tag{4}$$

Next, we define {0,1}-valued random variables $\{\chi_k, k = 0, \ldots, m\}$ as follows:

$$\begin{aligned} \chi_k &= 1, \text{ if } \tau_k < T \\ &= 0, \text{ else} \end{aligned} \tag{5}$$

By using this χ_k definition we get the desired factorization.

Proposition 3.1.
The reach probability satisfies the factorization:

$$\gamma = \prod_{k=1}^{m} \gamma_k \tag{6}$$

where $\gamma_k \triangleq E\{\chi_k = 1 \big| \chi_{k-1} = 1\} = \mathrm{P}(\tau_k < T \big| \tau_{k-1} < T)$.

Proof. Because $D_{k-1} \supset D_k$we have:

$$\inf\{t > 0;\ (\theta_t, x_t) \in D_{k-1} \vee t \geq T\} \leq \inf\{t > 0;\ (\theta_t, x_t) \in D_k \vee t \geq T\}$$

Substituting (4) at left and at right yields: $\tau_{k-1} \leq \tau_k$.

Hence we can derive:

$$\begin{aligned}
&\gamma = \mathrm{P}(\tau < T) = \mathrm{P}(\tau_m < T) \\
&= \mathrm{P}(\tau_m < T \wedge \tau_{m-1} \le \tau_m) = \mathrm{P}(\tau_m < T \wedge \tau_{m-1} < T) \\
&= P(\tau_m < T \mid \tau_{m-1} < T)\, P(\tau_{m-1} < T) \\
&= \prod_{k=1}^{m} \mathrm{P}(\tau_k < T \mid \tau_{k-1} < T)\, P(\tau_0 < T) \\
&= \prod_{k=1}^{m} \mathrm{P}(\tau_k < T \mid \tau_{k-1} < T) \\
&= \prod_{k=1}^{m} E\{\chi_k = 1 \mid \chi_{k-1} = 1\} = \prod_{k=1}^{m} \gamma_k \quad \square
\end{aligned}$$

3.3. Recursive estimation of the multi-level factors

By using the strong Markov property of $\{\theta_t, x_t\}$, we develop a recursive estimation of γ using the factorization in (6). First we define $\Xi' \triangleq \mathbb{R} \times \Xi$, $\xi_k \triangleq (\tau_k, \theta_{\tau_k}, x_{\tau_k})$, $Q_k \triangleq (0, T) \times D_k$, for $k = 1, \ldots, m$, and the following conditional probability measure $\pi_k(B)$ for an arbitrary Borel set B of Ξ':

$$\pi_k(B) \triangleq P(\xi_k \in B | \xi_k \in Q_k)$$

Cérou et al. [11] show that π_k is a solution of the following recursion of transformations:

$$\begin{array}{ccccc}
\pi_{k-1}(\cdot) & \xrightarrow{\text{I. mutation}} & p_k(\cdot) & \xrightarrow{\text{III. selection}} & \pi_k(\cdot) \\
 & & \downarrow{\scriptstyle \text{II. conditioning}} & & \\
 & & \gamma_k & &
\end{array}$$

where $p_k(B)$ is the conditional probability measure of $\xi_k \in B$ given $\xi_{k-1} \in Q_{k-1}$, i.e.,

$$p_k(B) \triangleq P(\xi_k \in B | \xi_{k-1} \in Q_{k-1})$$

Because $\{\theta_t, x_t\}$ is a strong Markov process, $\{\xi_k\}$ is a Markov sequence. Hence, the mutation transformation (I) satisfies a Chapman–Kolmogorov equation prediction for ξ_k:

$$p_k(B) = \int_{E'} p_{\xi_k|\xi_{k-1}}(B|\xi)\pi_{k-1}(d\xi) \text{ for all } B \in \beta(\Xi') \tag{7}$$

For the conditioning transformation (II) this means:

$$\gamma_k = \mathrm{P}(\tau_k < T | \tau_{k-1} < T) = \int_{E'} 1_{\{\xi \in Q_k\}} p_k(d\xi). \tag{8}$$

Hence, selection transformation (III) satisfies:

$$\pi_k(B) = \frac{\int_B 1_{\{\xi \in Q_k\}} p_k(d\xi)}{\int_{E'} 1_{\{\xi' \in Q_k\}} p_k(d\xi')} = [\int_B 1_{\{\xi \in Q_k\}} p_k(d\xi)]/\gamma_k. \tag{9}$$

With this, the γ_k terms in (6) are characterized as solutions of a recursive sequence of mutation Eq. (7), conditioning Eq. (8) and selection Eq. (9).

3.4. IPS algorithmic steps for a GSHS

Following Cérou et al. [11], Eqs. (6)–(9) yield the IPS algorithmic steps for the numerical estimation of γ :

$$\begin{array}{ccccccc}
\overline{\pi}_{k-1}(\cdot) & \xrightarrow{\text{I. mutation}} & \overline{p}_k(\cdot) & \xrightarrow{\text{III. selection}} & \tilde{\pi}_k(\cdot) & \xrightarrow{\text{IV. splitting}} & \overline{\pi}_k(\cdot) \\
 & & \downarrow{\scriptstyle \text{II. conditioning}} & & & & \\
 & & \overline{\gamma}_k & & & &
\end{array}$$

A set of N_P particles is used to form empirical density approximations $\overline{\gamma}_k$, $\overline{p}_k$ and $\overline{\pi}_k$ of γ_k, p_k and π_k respectively. By increasing the number N_P of particles in a set, the errors in these approximations decrease. When simulating particles from Q_{k-1} to Q_k, only a fraction $\overline{\gamma}_k$ of the simulated particle trajectories will reach Q_k within the time period $[0, T]$ considered; these particles form $\tilde{\pi}_k$. In order to start the next IPS cycle with N_P particles, the classical way is to perform a multinomial resampling (MR) of $\tilde{\pi}_k$ to produce $\overline{\pi}_k$. More effective splitting methods are: multinomial splitting (MS),

Algorithm 1; IPS-FAS algorithmic steps for a GSHS

Input: Initial measure π_0, end time T, decreasing sequence of closed subsets $D_k = \{(\theta_t, x_t) \in \Xi\}$, $D_{k-1} \supset D_k$, $k = 1,..,m$. Also $D_0 = \Xi$, $Q_k = (0,T) \times D_k$ and number of particles N_P.
Output: Estimated reach probability $\overline{\gamma}$

0. Initiation: Generate N_P particles $\xi_0^i \sim \pi_0$, $i = 1,..,N_P$, i.e. $\overline{\pi}_0(\cdot) = \sum_{i=1}^{N_P} \frac{1}{N_P} \delta_{\{\xi_0^i\}}(\cdot)$, with Dirac δ. Set $k = 1$.

I. Mutation: $\overline{p}_k(.) = \sum_{i=1}^{N_P} \frac{1}{N_P} \delta_{\{\overline{\xi}_k^i\}}(\cdot)$, where $\overline{\xi}_k^i$ is obtained by simulating the GSHS execution starting from ξ_{k-1}^i.

II. Conditioning: $\overline{\gamma}_k = \frac{N_{S_k}}{N_P}$ with $N_{S_k} = \sum_{i=1}^{N_P} 1(\overline{\xi}_k^i \in Q_k)$.

If $N_{S_k} = 0$, then $\overline{\gamma}_{k'} = 0, k' \in \{k,...,m\}$ and go to Step V.

III. Selection: $\tilde{\pi}_k(.) = \frac{1}{N_{S_k}} \sum_{i=1}^{N_{S_k}} \delta_{\{\tilde{\xi}_k^i\}}(\cdot)$,

with $\{\tilde{\xi}_k^j\}_{j=1}^{N_{S_k}}$ the collection of $\overline{\xi}_k^i \in Q_k$, $i = 1,..,N_P$.

IV. Splitting: $\{\tilde{\tilde{\xi}}_k^j\}_{j=1}^{N_{S_k}}$ is a random permutations of $\{\tilde{\xi}_k^j\}_{j=1}^{N_{S_k}}$.

Copy:
$$\xi_k^i = \tilde{\tilde{\xi}}_k^i \text{ for } i = 1,...,N_{S_k};$$
$$\xi_k^{N_{S_k}+i} = \tilde{\tilde{\xi}}_k^i \text{ for } i = 1,...,N_{S_k};$$
$$\cdots$$
$$\xi_k^{(\lfloor N_P/N_{S_k} \rfloor - 1)N_{S_k}+i} = \tilde{\tilde{\xi}}_k^i \text{ for } i = 1,...,N_{S_k};$$
$$\xi_k^{\lfloor N_P/N_{S_k} \rfloor N_{S_k}+i} = \tilde{\tilde{\xi}}_k^i \text{ for } i = 1,...,N_p - \lfloor N_p / N_{S_k} \rfloor N_{S_k}.$$

Each particle receives weight $1/N_p$.

V. If $k < m$, then $k := k+1$ and go to step I, else $\overline{\gamma} = \prod_{k=1}^{m} \overline{\gamma}_k$

residual multinomial splitting (RMS) and fixed assignment splitting (FAS). MS generates $\overline{\pi}_k$ by starting with the particles in $\tilde{\pi}_k$, and subsequently adding randomly selected particles from $\tilde{\pi}_k$ (with replacement). RMS first makes $\lfloor 1/\overline{\gamma}_k \rfloor$ copies from each particle in $\tilde{\pi}_k$, and subsequently complements the residual number $N_P \left(1 - \overline{\gamma}_k \lfloor 1/\overline{\gamma}_k \rfloor\right)$ by randomly selected particles from $\tilde{\pi}_k$ (with replacement). FAS also follows the two step approach of RMS, though during the second step the random selection from $\tilde{\pi}_k$ is done without replacement.

Cérou et al. [11] prove that using IPS with multinomial splitting (MS) for a strong hybrid state Markov process, $\overline{\gamma}$ forms an unbiased γ estimate, i.e.

$$\mathbb{E}\{\overline{\gamma}\} = \mathbb{E}\left\{\prod_{k=1}^{m} \overline{\gamma}_k\right\} = \prod_{k=1}^{m} \mathbb{E}\{\overline{\gamma}_k\} = \prod_{k=1}^{m} \gamma_k = \gamma \tag{10}$$

Moreover, Cérou et al. [11] derive second and higher order asymptotic bounds for the error $(\overline{\gamma} - \gamma)$ based on the multi-level Feynman–Kac analysis, e.g. [27, Theorem 12.2.2].

For a diffusion process $\{x_t\}$, Ma and Blom [43] have proven that IPS using FAS yields a lower or equal variance in the estimated reach probability $\overline{\gamma}$ than IPS using MR, MS or RMS. In the next section we extend these results for an IPS applied to a GSHS.

4. IPS algorithmic steps for GSHS

4.1. IPS application for a GSHS

The algorithmic steps of IPS application for a GSHS are specified in Algorithm 1 below. For the splitting step IV, use is made of FAS.

By extending the results of Ma and Blom [43] for IPS application to a diffusion, in Appendix we proof the following regarding the use of different splitting methods in IPS application to GSHS.

Algorithm 2. Simulating the execution of SHS transformed version of GSHS in step I of Algorithm 1

Input: i-th particle vector $\xi_{k-1}^i = (\tau_{k-1}^i, \theta_{k-1}^{*i}, x_{k-1}^{*i}, q_{k-1}^{*i})$, and the SHS elements $(\Theta^*, d^*, X^*, f^*, g^*, Init^*, R^*)$ and $Q_k^* = Q_k \times \mathbb{R}$.

Output: Estimated particle $\bar{\xi}_k^i = (\tau_k^i, \bar{\theta}_k^{*i}, \bar{x}_k^{*i}, \bar{q}_k^{*i})$

1. Set $t := \tau_{k-1}^i$ and $\bar{\varsigma} := (\theta_{k-1}^{*i}, x_{k-1}^{*i}, q_{k-1}^{*i})$
2. Evaluate equation (1) and $dq_t / dt = -\lambda(\theta_t, x_t)$ from $\bar{\varsigma}$ at t until $t_+ = \min\{t + \triangle, \bar{s}_t, \bar{\tau}_k\}$; this yields $\bar{\varsigma}_+$. Here $\bar{s}_t$ is the first time $> t$ that this solution hits the boundary of X^*; and $\bar{\tau}_k$ is the first time that this solution hits Q_k^*.
3. If $t_+ \geq \bar{\tau}_k$ then stop with output $\bar{\xi}_k^i = (\bar{\tau}_k, \bar{\theta}_k^{*i}, \bar{x}_k^{*i}, \bar{q}_k^{*i})$, where $(\bar{\theta}_k^{*i}, \bar{x}_k^{*i}, \bar{q}_k^{*i}) \sim R^*(\bar{\varsigma}_+, .)$ if $\bar{s}_t = \bar{\tau}_k$, else $(\bar{\theta}_k^{*i}, \bar{x}_k^{*i}, \bar{q}_k^{*i}) := \bar{\varsigma}_+$.
4. If $t_+ \geq \bar{s}_t$ then $\bar{\varsigma} \sim R^*(\bar{\varsigma}_+, .)$, set $t := t_+$ and repeat from step 2.

Theorem 4.1. *Replacing the FAS splitting step IV in algorithm 1 by RMS splitting, MS splitting or MR splitting has the following effects on the variance* $\mathrm{V}\{\overline{\gamma}\}$*:*

$$\mathrm{V}_{FAS}\{\overline{\gamma}\} \leq \mathrm{V}_{RMS}\{\overline{\gamma}\} \leq \mathrm{V}_{MS}\{\overline{\gamma}\} \leq \mathrm{V}_{MR}\{\overline{\gamma}\} \tag{11}$$

Proof. See Appendix.

Next we address the details of mutation step I of Algorithm 1, i.e. the Monte Carlo simulation of the GSHS from particle state ξ_{k-1}^i to particle state $\bar{\xi}_k^i$. Section 4.2 addresses simulation of the execution of an SHS transformed version of GSHS within IPS. Section 4.3 develops an algorithm that takes into account that the "remaining local time" process $\{q_t^*\}$ should be unobservable for the IPS process. For reference purpose, Section 4.3 addresses the more demanding direct simulation of the execution of a GSHS, i.e. without using the transformation to SHS.

4.2. Simulation of execution of SHS transformed version of GSHS in mutation step I

The process $\{\theta_t, x_t\}$ is assumed to be the SHS transformed version of the GSHS, i.e. $\{\theta_t, x_t\} = \{\theta_t^*, x_t^*, q_t^*\}$ as defined in Section 2.3. Then in step I of Algorithm 1, the evolution of $\{\theta_t, x_t\} = \{\theta_t^*, x_t^*, q_t^*\}$ is executed on interval $[\tau_{k-1}^i, \tau_k^i]$, starting with ξ_{k-1}^i and delivering ξ_k^i. Mutation step I is conducted using Euler–Maruyama integration of Eq. (1) along small time steps $\triangle$, i.e.

$$\begin{aligned} \theta_{t+\triangle} &= \theta_t \\ x_{t+\triangle} &= f(\theta_t, x_t)\triangle + g(\theta_t, x_t)(W_{t+\triangle} - W_t) \end{aligned} \tag{12}$$

The algorithm for the execution of an SHS transformed version of GSHS within mutation step I is specified below.

Remark. Convergence of the Euler–Maruyama integration scheme (12) is guaranteed iff the SDE coefficients satisfy certain Lipschitz conditions, e.g. [44].

If during any of the small time steps $\triangle$ one of the boundaries of X^* or Q_k^* is passed, then additional MC simulation steps may be conducted to get a better approximation $\bar{s}_t$ or $\bar{\tau}_k$ of the first hitting time. As an alternative for using a lower $\triangle$ value, Glasserman [45, p. 367] proposes an interpolation of the solution of Eq. (1) on the $\triangle$ interval considered, by simulating a Brownian bridge between the already simulated Brownian motion points W_t and $W_{t+\triangle}$. The resulting Brownian bridge yields a more accurate approximation of the first hitting time.

4.3. Accounting for unobservability of remaining local time

As has been identified at the end of Section 2.4, the "remaining local time" process $\{q_t^*\}$ of the SHS transformed version of a GSHS should be treated as being unobservable for the IPS process. To formalize this, the transformation to SHS is applied to a enriched version of the original GSHS. The GSHS enrichment consists of adding IPS hitting levels Q_k, $k = 1, \ldots, m$, to the original GSHS, with reset $(\theta_{\tau_k}, x_{\tau_k}) = (\theta_{\tau_k -}, x_{\tau_k -})$, at a hitting time τ_k. Thanks to the continuity of the latter reset, the execution of the enriched GSHS yields the same pathwise solutions as execution of the original GSHS does. Subsequent application of the transformation of Lygeros and Prandini [7] to this enriched GSHS yields a SHS,

Algorithm 3. Simulating execution of SHS version of modified GSHS in step I of Algorithm 1

Input: i-th particle vector $\xi^i_{k-1} = (\tau^i_{k-1}, \theta^{*i}_{k-1}, x^{*i}_{k-1}, q^{*i}_{k-1})$, and the SHS elements $(\Theta^*, d^*, X^*, f^*, g^*, Init^*, R^*)$ and $\mathcal{Q}^*_k = \mathcal{Q}_k \times \mathbb{R}$.

Output: Estimated particle $\bar{\xi}^i_k = (\tau^i_k, \bar{\theta}^{*i}_k, \bar{x}^{*i}_k, \bar{q}^{*i}_k)$

1. Set $t := \tau^i_{k-1}$ and $\bar{\varsigma} := (\theta^{*i}_{k-1}, x^{*i}_{k-1}, \bar{q})$, with $\bar{q} \sim \exp(1)$
2. = step 2 in algorithm 2.
3. = step 3 in algorithm 2.
4. = step 4 in algorithm 2.

Algorithm 4. Simulating GSHS execution (step I of algorithm 1)

Input: i-th particle vector $\xi^i_{k-1} = (\tau^i_{k-1}, \theta^i_{k-1}, x^i_{k-1})$, $\mathcal{Q}_k$, the GSHS elements $(\Theta, d, X, f, g, Init, \lambda, R)$, and the transition rate maximum $\bar{\lambda}$.

Output: Estimated particle $\bar{\xi}^i_k = (\bar{\tau}^i_k, \bar{\theta}^i_k, \bar{x}^i_k)$

1. Set $t = \tau^i_{k-1}$ and $\bar{\varsigma} := (\theta^i_{k-1}, x^i_{k-1})$
2. Generate $u \sim \mathrm{U}(0,1)$, and set $\Delta_t := -(\ln u)/\bar{\lambda}$
3. Evaluate equation (1) from $\bar{\varsigma}$ at t until $t_+ = \min\{t + \triangle, t + \Delta_t, \bar{s}_t, \bar{\tau}_k\}$; this yields $\bar{\varsigma}_+$. Here $\bar{s}_t$ is the first time $> t$ that this solution hits the boundary of X; and $\bar{\tau}_k$ is the first time that this solution hits $\mathcal{Q}_k$.
4. If $t_+ \geq \bar{\tau}_k$ then stop with output $\bar{\xi}^i_k = (\bar{\tau}^i_k, \bar{\theta}^i_k, \bar{x}^i_k)$, where $(\bar{\theta}^i_k, \bar{x}^i_k) \sim R(\bar{\varsigma}_+, .)$ if $\bar{s}_t = \bar{\tau}_k$, else $(\bar{\theta}^i_k, \bar{x}^i_k) := \bar{\varsigma}_+$
5. If $t_+ \geq \bar{s}_t$ then $\bar{\varsigma} \sim R(\bar{\varsigma}_+, .)$, set $t := t_+$ and repeat from step 2
6. If $t_+ \geq t + \Delta_t$ then generate $v \sim \mathrm{U}(0,1)$
7. If $\lambda(\bar{\varsigma}_+) \geq v\bar{\lambda}$, then generate $\bar{\varsigma} \sim R(\bar{\varsigma}_+, (.,.))$, else $\bar{\varsigma} := \bar{\varsigma}_+$
8. Set $t := t_+$ and repeat from step 2.

that also resets the remaining local time upon reaching an IPS hitting level Q_k, $k = 1, \ldots, m$. For algorithm 2 this means that it can be improved by adding a reset of local remaining time at the beginning of each IPS cycle; this is specified in algorithm 3 below. Hence, at the begin of mutation step I within an IPS cycle, the remaining local time value of each particle is freshly sampled from exp (1).

The combination of algorithms 1&3 starts at each IPS cycle with N_p particles, each of which has a different sample of remaining local time q^{*i}_{k-1}, $k = 1, ..m$. This differs significantly from the combination of algorithm combination 1&2, where the N_p particles having different remaining local time ${q_0}^{*i}$ applies at the start of the first IPS cycle only. Hence, with increasing IPS level k, under algorithm combination 1&3 particle diversity will gain relative to particle diversity under algorithm combination 1&2.

4.4. Simulation of original GSHS execution in mutation step I

For reference purpose, we also specify an algorithm for the simulation of the original GSHS execution. For this we follow the numerical integration scheme of Krystul ([41], Chapter 4). In addition to fixed small time steps $\triangle$, random time steps are generated at which potential jumps may happen. Realizations of the these random time steps are obtained through Monte Carlo sampling of an in-homogeneous Poisson process on $[0, T] \times \left[0, \bar{\lambda}\right]$, with $\bar{\lambda} \geq \sup_{(\theta,x)\in\Xi} \lambda(\theta, x)$. Subsequently the potential Poisson points are thinned by rejecting points that lie above the graph of $\lambda(\theta_t, x_t)$. The remaining points, i.e., those at or below the graph of $\lambda(\theta_t, x_t)$, are projected onto the *time*-axis $[0, T]$. The resulting execution of the GSHS within an IPS cycle, starting from ξ^i_{k-1}, on the interval $[\tau^i_{k-1}, \tau^i_k]$ is specified in algorithm 4.

In case of a stop during step 4 of GSHS algorithm 4, there is a "remaining integration time" $t + \Delta_t - \bar{\tau}_k$. Because this "remaining integration time" does not make part of the Markov state $\xi_{\bar{\tau}_k}$, it does not influence the GSHS execution during the next IPS cycle. The latter coincides with ignoring "remaining local time" in algorithm 3. Hence it is expected that algorithm combination 1&4 estimates reach probability similarly well as algorithm combination 1&3 does.

Table 1
Analytical γ results for various μ.

μ (s)	γ
0.9	5.19976×10^{-4}
0.8	6.97696×10^{-5}
0.7	3.72665×10^{-6}
0.6	4.08284×10^{-8}

5. Application of IPS to GSHS example

5.1. Hypothetical car example

A car driver in dense fog is heading to a wall at position d_{wall}. If the car is at distance d_{fog} from the wall, then the driver sees the wall for the first time. Then, it takes the driver a random reaction delay to start braking, with a density $p_{delay}(s)$. During the reaction delay, the velocity of the car does not change; after the reaction delay, the car decelerates at constant value $a_{\min}$. The aim is to estimate the probability γ that the car hits the wall.

From the moment that the car reaches distance d_{fog} from the wall at velocity v_0, it takes the sum of reaction delay T_{delay} and the time of deceleration $T_{dec} = -v_0/a_{\min}$ until the car is at a standstill. This implies

$$\gamma = \mathrm{P}\{v_0 T_{delay} + v_0 T_{dec} + \frac{1}{2} a_{\min} T_{dec}^2 \geq d_{fog}\} \tag{13}$$

Elaboration of (13) yields:

$$\gamma = \mathrm{P}\{T_{delay} \geq \frac{1}{2} v_0/a_{\min} + d_{fog}/v_0\} \tag{14}$$

If we assume a Rayleigh density $p_{delay}(s) = \frac{s}{\mu^2} e^{-s^2/(2\mu^2)}$, and we write $T_C = \frac{1}{2} v_0/a_{\min} + d_{fog}/v_0$, evaluation of (14) yields:

$$\gamma = \int_{T_C}^{+\infty} \frac{t}{\mu^2} e^{-t^2/(2\mu^2)} dt = -e^{-t^2/(2\mu^2)}\Big|_{t=T_C}^{+\infty} = e^{-t^2/(2\mu^2)}|_{t=T_C} \tag{15}$$

Table 1 gives the analytically obtained γ results for various mean reaction delays μ, and parameter settings $d_{wall} =$ 300 m, $d_{fog} = 120$ m, $v_0 = 72$ km/h $= 20$ m/s, $a_{\min} = -4$ m/s^2.

For this example, Section 5.2 specifies the GSHS model and the transformation of Section 2.4 to an SHS model. Section 5.3 estimates γ using straightforward MC simulation and IPS-FAS algorithm combinations 1&2, 1&3 and 1&4.

5.2. GSHS model and transformation to SHS model

For this example, the discrete set of the GSHS is:

$$\Theta = \{-1, 0, delay, stop, hit\} \tag{16}$$

where -1 indicates decelerating mode, 0 indicates uniform mode, *delay* is a reaction delay mode, *stop* indicates stopping mode, and *hit* indicates the wall has been hit. A transition diagram representing the transitions between these modes is given in Fig. 1.

The continuous state components are $x_t = Col(z_t, y_t, v_t)$, where z_t is the amount of time passed since the driver could see the wall for the first time, y_t is the position of the car at time t, and v_t is the velocity at time t. Hence, the dimension of the continuous state space is $d(.) = 3$. The subsets X^θ are defined as follows:

$$\begin{aligned} X^0 &= \mathbb{R} \times (-\infty, d_{wall} - d_{fog}) \times \mathbb{R} \\ X^{-1} &= \mathbb{R} \times (-\infty, d_{wall}) \times (0, \infty) \\ X^{delay} &= \mathbb{R} \times (-\infty, d_{wall}) \times \mathbb{R} \\ X^{stop} &= \mathbb{R} \times (-\infty, d_{wall}) \times 0 \\ X^{hit} &= \mathbb{R}^3 \end{aligned} \tag{17}$$

The initial measure *Init* generates $\theta_0 = 0, z_0 = 0, y_0 = 0$. Between switching moment of $\{\theta_t\}$, x_t evolves as (1) with $f\left(\theta, [z, y, v]^T\right) = [1, v, 1\{\theta = -1\}a_{\min}]^T$ and $g(\theta, .) = [0, g_2, 0]^T$ if $\theta \in \{0, delay, -1\}$, else $g(\theta, .) = [0, 0, 0]^T$. The analytical results in Table 1 apply for $g_2 = 0$, i.e. no Brownian motion.

The instantaneous transition rate $\lambda(\theta_t, (z_t, y_t, v_t))$ satisfies:

$$\lambda(\theta, (z, y, v)) = \chi(\theta = delay) p_{delay}(z) / \int_z^\infty p_{delay}(s) ds \tag{18}$$

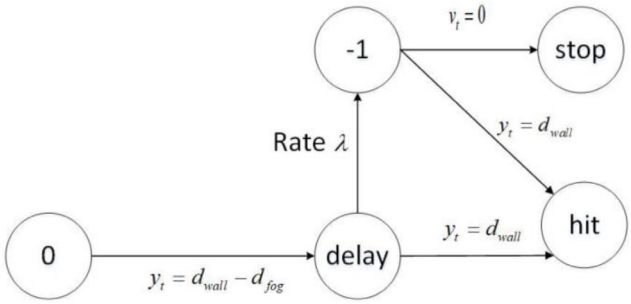

Fig. 1. State transition diagram of GSHS model.

The transition measure $R((\theta,(z,y,v)),(.,.))$ satisfies:

$R((-1,(z,y,v)),\{stop\}\times\{0,y,v\}) = 1$ iff $v = 0$

$R((0,(z,y,v)),\{delay\}\times\{0,y,v\}) = 1$ iff $y = d_{wall} - d_{fog}$

$R((delay,(z,y,v)),\{-1\}\times\{0,y,v\}) = 1$, iff λ generates a point ,

$R((delay,(z,y,v)),\{hit\}\times\{0,y,0\}) = 1$, iff $y = d_{wall}$

$R((-1,(z,y,v)),\{hit\}\times\{0,y,0\}) = 1$, iff $y = d_{wall}$..

IPS-FAS algorithm combination 1&4 makes use of this GSHS model. By applying the transformation from Section 2.3, the above GSHS model transforms to an SHS model. The resulting SHS has continuous state components (z_t, y_t, v_t, q_t), with $\{q_t\}$ evolving as $dq_t = -\lambda(\theta_t,(z_t,y_t,v_t))dt$ in between discontinuities, and $q_s \sim \exp(1)$ at a mode switch and if q_{t-} hits 0.

IPS-FAS algorithm combinations 1&2 and 1&3 make use of this SHS transformed version of the GSHS model. Though algorithm combination 1&3 also refreshes the "remaining time" q_{τ_k-} at the start of a mutation during the next IPS cycle.

5.3. Simulation results

By conducting each of the approaches $N_{\overline{\gamma}}$ times we get $\overline{\gamma}^i, i = 1,\ldots,N_{\overline{\gamma}}$. These results are used to assess the mean $\hat{\gamma}$, the percentage ρ_S of successful IPS runs, and the normalized root-mean-square error (RMSE), i.e.

$$\hat{\gamma} = \frac{1}{N_{\overline{\gamma}}}\sum_{i=1}^{N_{\overline{\gamma}}}\overline{\gamma}^i \tag{19}$$

$$\rho_S = \frac{1}{N_{\overline{\gamma}}}\sum_{i=1}^{N_{\overline{\gamma}}}1(\overline{\gamma}^i > 0) \tag{20}$$

$$RMSE = \sqrt{\frac{1}{N_{\overline{\gamma}}}\sum_{i=1}^{N_{\overline{\gamma}}}(\overline{\gamma}^i - \gamma)^2} \tag{21}$$

In the subsequent IPS cycles the following levels are used: $D_k = \{0, delay, hit\}\times\mathbb{R}\times[L_k,\infty)\times\mathbb{R}\cup\{-1, stop\}\times\mathbb{R}\times[d_{wall},\infty)\times\mathbb{R}$, with the μ-dependent L_k values shown in Table 2.

For $g_2 = 0$ and $g_2 = 1$, Tables 3 and 4 respectively show simulation results of straightforward MC and of IPS-FAS using algorithm combinations 1&2, 1&3 and 1&4. These results show that IPS-FAS combination 1&2 performs similar or slightly better than straightforward MC simulation. Both in Table 3 and in Table 4, IPS-FAS combinations 1&3 and 1&4 perform far better than MC and IPS-FAS combination 1&2.

For $g_2 = 0$ and $\mu = 0.8$ s, Tables 5, 6 and 7 present average counts of particles per IPS level, over successful IPS-FAS runs of algorithm combinations 1&2, 1&3 and 1&4 respectively. Comparison of Tables 5 and 6 show a steady increase in particle diversity under algorithm combination 1&3 relative to combination 1&2. Comparison of Tables 6 and 7 show that diversity of particles after mutation step I is similar under algorithm combinations 1&3 and 1&4.

For the GSHS example $g_2 = 0, \mu = 0.8$ s, the differences in particle diversity in Tables 5–7 correspond with the theory-based expectations in Sections 4.3 and 4.4.

Table 2
Values of L_k for various μ values.

k	μ			
	0.9 s	0.8 s	0.7 s	0.6 s
1	181	181	181	181
2	217	215	210	205
3	230	230	220	215
4	240	241	230	223
5	300	300	237	230
6			244	236
7			300	243
8				300

Table 3
Simulation results for MC and IPS-FAS algorithm combinations 1&2, 1&3 and 1&4 applied to the GSHS example $g_2 = 0$ at simulation settings $\Delta = 0.01$ s, $N_p = 1000$, and $N_{\overline{\gamma}} = 100$.

$\mu = 0.9$ s	$\hat{\gamma}$	ρ_S	$RMSE/\gamma$
MC (m = 1)	5.300×10^{-4}	44%	137.2%
IPS-FAS combination 1&2	3.859×10^{-4}	33%	116.7%
IPS-FAS combination 1&3	5.096×10^{-4}	100%	13.4%
IPS-FAS combination 1&4	5.125×10^{-4}	100%	15.2%
$\mu = 0.8$ s	$\hat{\gamma}$	ρ_S	$RMSE/\gamma$
MC (m = 1)	4.000×10^{-5}	4%	284.1%
IPS-FAS combination 1&2	3.811×10^{-5}	4%	271.7%
IPS-FAS combination 1&3	6.968×10^{-5}	100%	20.6%
IPS-FAS combination 1&4	6.948×10^{-5}	100%	19.8%
$\mu = 0.7$ s	$\hat{\gamma}$	ρ_S	$RMSE/\gamma$
MC (m = 1)	/	/	/
IPS-FAS combination 1&2	/	/	/
IPS-FAS combination 1&3	3.605×10^{-6}	100%	20.9%
IPS-FAS combination 1&4	3.757×10^{-6}	100%	20.4%
$\mu = 0.6$ s	$\hat{\gamma}$	ρ_S	$RMSE/\gamma$
MC (m = 1)	/	/	/
IPS-FAS combination 1&2	/	/	/
IPS-FAS combination 1&3	4.055×10^{-8}	100%	28.30%
IPS-FAS combination 1&4	4.029×10^{-8}	100%	28.47%

Table 4
Simulation results for MC and IPS-FAS algorithm combinations 1&2, 1&3 and 1&4 applied to the GSHS example $g_2 = 1$ at simulation settings $\Delta = 0.01$ s, $N_p = 1000$, and $N_{\overline{\gamma}} = 100$.

$\mu = 0.9$ s	$\hat{\gamma}$	ρ_S	$RMSE/\hat{\gamma}$
MC (m = 1)	7.000×10^{-4}	50%	120.37%
IPS-FAS combination 1&2	6.306×10^{-4}	94%	110.11%
IPS-FAS combination 1&3	6.829×10^{-4}	100%	13.95%
IPS-FAS combination 1&4	6.832×10^{-4}	100%	15.60%
$\mu = 0.8$ s	$\hat{\gamma}$	ρ_S	$RMSE/\hat{\gamma}$
MC (m = 1)	4.000×10^{-5}	3%	604.15%
IPS-FAS combination 1&2	1.266×10^{-4}	49%	244.33%
IPS-FAS combination 1&3	1.027×10^{-4}	100%	18.62%
IPS-FAS combination 1&4	1.022×10^{-4}	100%	17.37%
$\mu = 0.7$ s	$\hat{\gamma}$	ρ_S	$RMSE/\hat{\gamma}$
MC (m = 1)	1.000×10^{-5}	1%	994.99%
IPS-FAS combination 1&2	1.316×10^{-5}	14%	666.32%
IPS-FAS combination 1&3	6.921×10^{-6}	100%	16.52%
IPS-FAS combination 1&4	7.021×10^{-6}	100%	18.93%
$\mu = 0.6$ s	$\hat{\gamma}$	ρ_S	$RMSE/\hat{\gamma}$
MC (m = 1)	/	/	/
IPS-FAS combination 1&2	/	/	/
IPS-FAS combination 1&3	1.199×10^{-7}	100%	28.34%
IPS-FAS combination 1&4	1.140×10^{-7}	100%	25.39%

Table 5
Average counts of particles per level over successful IPS-FAS runs of combination 1&2, for $g_2 = 0, \mu = 0.8$ s.

k	No. of particles at start of Step I	No. of different particles at start of Step I	No. of different particles after Step I	No. of survived particles after Step III	No. of different particles after Step III	% of successful IPS runs through level k
1	1000	1	999.99	997.96	997.96	100%
2	1000	997.96	971.46	92.84	92.62	100%
3	1000	92.62	92.15	82.58	7.59	100%
4	1000	7.59	13.26	184.40	1.41	49%
5	1000	1.41	18.51	592.16	1	6%

Table 6
Average counts of particles per level over successful IPS-FAS runs of combination 1&3, for $g_2 = 0, \mu = 0.8$ s.

k	No. of particles at start of Step I	No. of different particles at start of Step I	No. of different particles after Step I	No. of survived particles after Step III	No. of different particles after Step III	% of successful IPS runs through level k
1	1000	1	999.98	998.25	998.25	100%
2	1000	998.25	974.03	92.14	92.14	100%
3	1000	92.14	929.76	82.10	82.10	100%
4	1000	82.10	906.45	92.28	92.28	100%
5	1000	92.28	889.19	100.17	98.80	100%

Table 7
Average counts of particles per level over successful IPS-FAS runs using combination 1&4, for $g_2 = 0, \mu = 0.8$ s.

k	No. of particles at start of Step I	No. of different particles at start of Step I	No. of different particles after Step I	No. of survived particles after Step III	No. of different particles after Step III	% of successful IPS runs through level k
1	1000	1	3.15	997.85	1	100%
2	1000	1	909.74	91.26	1	100%
3	1000	1	917.58	83.42	1	100%
4	1000	1	908.38	92.62	1	100%
5	1000	1	999.41	99.01	98.42	100%

For the GSHS example $g_2 = 1, \mu = 0.8$ s, in addition to random delays, Brownian motion creates small differences in the position component of particles, as a result of which almost all particles will differ from each other. As shown in Table 4, in spite of this Brownian motion effect, algorithm combination 1&2 falls short in capturing proper effect on particle diversity and reach probability by the spontaneous jumps in the original GSHS.

6. Conclusion

In many application domains, processes have a hybrid state space and their evolution involves diffusion as well as forced and spontaneous jumps. This explains why GSHS and its subclasses play a key role in formal modeling and analysis. However in simulation and control of such systems, common practice is to use an SHS model, i.e. a hybrid system that involves diffusion and forced jumps, though no spontaneous jumps. Hence a relevant question is: "Can a GSHS model be transformed to an SHS model without changing process behavior that is relevant for the application considered?" This paper has addressed this question in using the Interacting Particle System (IPS) framework of Cérou et al. [11] for numerically estimating the reach probability γ of an unsafe set D in a GSHS model.

In Section 2 stochastic process executions of GSHS have been defined, as well as their relation to solutions of SDE's on a hybrid space. Also explained is that the transformation of GSHS to an SHS by Lygeros and Prandini [7] has as side-effect that it produces "remaining local time" information that should be treated as being not observable for other process(es) than the GSHS execution considered.

Section 3 explains the IPS setting for a GSHS, by adopting a nested sequence of increasing subsets of D, and an implied factorization of the reach probability γ. Because a GSHS may jump over a subset boundary it is shown that this does not hinder the factorization (Proposition 3.1).

Section 4 develops IPS algorithms for application to GSHS. First, Section 4.1 specifies the IPS algorithm cycles for a GSHS using Fixed Assignment Splitting (FAS). Theorem 4.1 proves that this yields lower or equal variance than using other IPS with splitting options. Section 4.2 addresses IPS evaluation of a GSHS by using an SHS version, that follows from the Lygeros and Prandini [7] transformation. The side-effect is that each IPS cycle makes use of the "remaining local time" information that is non-existing in the original GSHS. Section 4.3 mitigates this side-effect, by an enrichment of

the original GSHS, prior to applying the transformation of Lygeros and Prandini [7] with the first hitting times of the IPS subsets. Thanks to this enrichment, the resulting SHS refreshes "remaining local time" at the start of each next IPS cycle. The latter refreshment induces a significant improvement in particle diversity at the start of each IPS cycle. As a result of this improved particle diversity IPS performance in reach probability estimation is expected to significantly improve when reach probability estimation becomes a challenge. For purpose of comparison, in Section 4.4 an algorithm for the direct simulation of a GSHS execution within IPS cycles is specified. Based on theory, use of this algorithm in IPS for GSHS will yield similar good performance as the algorithm of Section 4.3. In Section 5, the expected differences in IPS performance have been illustrated for a GSHS example.

The findings in Section 4 mean that for IPS based reach probability estimation for an arbitrary GSHS model, can be applied to a properly derived SHS version of the GSHS model. The proper way in deriving such SHS consists of three steps. The first step is to specify a GSHS model of the practical system. The second step is to enrich this GSHS with the first hitting times of the IPS subsets, without affecting the pathwise behavior of the GSHS execution. The third step is to apply the transformation by Lygeros and Prandini [7] to the enriched GSHS from step 2.

In view of this positive finding for the limited scope of IPS application to GSHS, a logical follow-on question is if there also exists an improved transformation of a GSHS to SHS for stochastic control problems. Such transformation would make optimal control policies developed for SHS applicable to GSHS.

CRediT authorship contribution statement

Hao Ma: Investigation, Formal analysis, Methodology, Software, Validation, Writing – original draft, Writing – review & editing. **Henk A.P. Blom:** Conceptualization, Investigation, Formal analysis, Methodology, Writing – original draft, Writing – review & editing, Supervision.

Declaration of competing interest

The authors declare that they have no known competing financial interests or personal relationships that could have appeared to influence the work reported in this paper.

Acknowledgments

The authors would like to thank anonymous reviewers for helpful suggestions in improving the paper, and Bert Bakker (NLR, Amsterdam) for suggesting the comparison of GSHS and SHS in applying IPS.

Appendix. Proof of Theorem 4.1

In this appendix we compare the variance of applying IPS to GSHS under FAS versus multinomial resampling (MR), multinomial splitting (MS), and residual multinomial splitting (RMS). In doing so it becomes clear that the earlier comparison by Ma and Blom [43] for diffusion process extends to GSHS executions.

The first proof starts with a characterization of the conditional distribution of particles that reach level $k+1$, given that at level k the ith successful particle $\tilde{\xi}_k^i$ is copied K_k^i times, $i = 1, \ldots, N_{S_k}$.

Proposition A.1. *If $N_{S_k} > 0$ and K_k^i, with $i = 1, 2, \ldots, N_{S_k}$, denote the number of particles that copies $\tilde{\xi}_k^i$ at level k. Then the number $Y_{k+1}^{k,i}$, of the K_k^i particle copies of $\tilde{\xi}_k^i$ that reach level k+1, has a conditional Binomial distribution of size K_k^i and success probability $\gamma_{k+1}(\tilde{\xi}_k^i)$, i.e.*

$$p_{Y_{k+1}^{k,i}|K_k^i,\tilde{\xi}_k^i}(n; K_k^i, \tilde{\xi}_k^i) = \mathrm{Bin}(n; K_k^i, \gamma_{k+1}(\tilde{\xi}_k^i)) \tag{22}$$

with

$$\gamma_{k+1}(\tilde{\xi}_k^i) \triangleq \mathrm{P}(\tau_{k+1} < T | \xi_k = \tilde{\xi}_k^i) \tag{23}$$

Proof. Similar to the proof of Proposition 1 in [43].

Theorem A.1. *If $N_{S_k} \geq 1$ and K_k^i, $i = 1, ..N_{S_k}$, denotes the number of copies made of the ith successful particle $\tilde{\xi}_k^i$ during the splitting step at level k of the IPS algorithm, then*

$$\mathbb{E}\left\{\overline{\gamma}_{k+1}|\tilde{\xi}_k^j, \text{ all}\, j\right\} = \frac{1}{N_p}\sum_{i=1}^{N_{S_k}}\left[\mathbb{E}\left\{K_k^i|\tilde{\xi}_k^j, \text{ all}\, j\right\}\gamma_{k+1}(\tilde{\xi}_k^i)\right] \tag{24}$$

$$
\begin{aligned}
&\mathrm{Var}\left\{\overline{\gamma}_{k+1}|\tilde{\xi}_k^j,\ \mathrm{all}\, j\right\}\\
&=\frac{1}{N_p^2}\sum_{i=1}^{N_{S_k}}\left[\mathbb{E}\left\{K_k^i|\tilde{\xi}_k^j,\ \mathrm{all}\, j\right\}\gamma_{k+1}(\tilde{\xi}_k^i)\left(1-\gamma_{k+1}(\tilde{\xi}_k^i)\right)\right]\\
&+\frac{1}{N_p^2}\sum_{i=1}^{N_{S_k}}\left[\mathrm{Var}\left\{K_k^i|\tilde{\xi}_k^j,\ \mathrm{all}\, j\right\}\gamma_{k+1}(\tilde{\xi}_k^i)^2\right]\\
&+\frac{1}{N_p^2}\sum_{i=1}^{N_{S_k}}\sum_{\substack{i'=1\\ i'\neq i}}^{N_{S_k}}\left[\mathrm{Cov}\left\{K_k^i,K_k^{i'}|\tilde{\xi}_k^j,\ \mathrm{all}\, j\right\}\gamma_{k+1}(\tilde{\xi}_k^i)\,\gamma_{k+1}(\tilde{\xi}_k^{i'})\right]
\end{aligned}
\tag{25}
$$

Proof. Similar to the proof of Theorem 1 in [43].

Proposition A.2. *If $N_{S_k}\geq 1$, and we use multinomial resampling at IPS level k then*

$$
\mathbb{E}\left\{\overline{\gamma}_{k+1}|\tilde{\xi}_k^1,\ldots,\tilde{\xi}_k^{N_{S_k}}\right\}=\frac{1}{N_{S_k}}\sum_{i=1}^{N_{S_k}}\gamma_{k+1}(\tilde{\xi}_k^i)
\tag{26}
$$

$$
\begin{aligned}
&\mathrm{Var}\left\{\overline{\gamma}_{k+1}|\tilde{\xi}_k^1,\ldots,\tilde{\xi}_k^{N_{S_k}}\right\}\\
&=\frac{1}{N_pN_{S_k}}\sum_{i=1}^{N_{S_k}}\left[\gamma_{k+1}(\tilde{\xi}_k^i)\left(1-\gamma_{k+1}(\tilde{\xi}_k^i)\right)\right]\\
&+\frac{1}{N_pN_{S_k}}\left[\sum_{i=1}^{N_{S_k}}\left[\left(\gamma_{k+1}(\tilde{\xi}_k^i)\right)^2\right]-\frac{1}{N_{S_k}}\sum_{i=1}^{N_{S_k}}\sum_{i'=1}^{N_{S_k}}\left[\left(\gamma_{k+1}(\tilde{\xi}_k^i)\gamma_{k+1}(\tilde{\xi}_k^{i'})\right)\right]\right]
\end{aligned}
\tag{27}
$$

Proof. Similar to the proof of Proposition 2 in [43].

Proposition A.3. *If $N_{S_k}\geq 1$, and we use multinomial splitting at IPS level k then*

$$
\mathbb{E}\left\{\overline{\gamma}_{k+1}|\tilde{\xi}_k^1,\ldots,\tilde{\xi}_k^{N_{S_k}}\right\}=\frac{1}{N_{S_k}}\sum_{i=1}^{N_{S_k}}\gamma_{k+1}(\tilde{\xi}_k^i)
\tag{28}
$$

$$
\begin{aligned}
&\mathrm{Var}\left\{\overline{\gamma}_{k+1}|\tilde{\xi}_k^1,\ldots,\tilde{\xi}_k^{N_{S_k}}\right\}\\
&=\frac{1}{N_pN_{S_k}}\sum_{i=1}^{N_{S_k}}\left[\gamma_{k+1}(\tilde{\xi}_k^i)\left(1-\gamma_{k+1}(\tilde{\xi}_k^i)\right)\right]\\
&+\frac{(N_p-N_{S_k})}{{N_p}^2N_{S_k}}\left[\sum_{i=1}^{N_{S_k}}\left[\left(\gamma_{k+1}(\tilde{\xi}_k^i)\right)^2\right]-\frac{1}{N_{S_k}}\sum_{i=1}^{N_{S_k}}\sum_{i'=1}^{N_{S_k}}\left[\gamma_{k+1}(\tilde{\xi}_k^i)\gamma_{k+1}(\tilde{\xi}_k^{i'})\right]\right]
\end{aligned}
\tag{29}
$$

Proof. Similar to the proof of Proposition 3 in [43].

Proposition A.4. *If $N_{S_k}\geq 1$, and we use residual multinomial splitting at IPS level k then*

$$
\mathbb{E}\left\{\overline{\gamma}_{k+1}|\tilde{\xi}_k^1,\ldots,\tilde{\xi}_k^{N_{S_k}}\right\}=\frac{1}{N_{S_k}}\sum_{i=1}^{N_{S_k}}\gamma_{k+1}(\tilde{\xi}_k^i)
\tag{30}
$$

$$
\begin{aligned}
&\mathrm{Var}\left\{\overline{\gamma}_{k+1}|\tilde{\xi}_k^1,\ldots,\tilde{\xi}_k^{N_{S_k}}\right\}\\
&=\frac{1}{N_pN_{S_k}}\sum_{i=1}^{N_{S_k}}\left[\gamma_{k+1}(\tilde{\xi}_k^i)\left(1-\gamma_{k+1}(\tilde{\xi}_k^i)\right)\right]+\frac{\left(N_p \bmod N_{S_k}\right)}{N_p^2N_{S_k}}\\
&\cdot\left[\sum_{i=1}^{N_{S_k}}\left[\left(\gamma_{k+1}(\tilde{\xi}_k^i)\right)^2\right]-\frac{1}{N_{S_k}}\sum_{i=1}^{N_{S_k}}\sum_{i'=1}^{N_{S_k}}\left[\left(\gamma_{k+1}(\tilde{\xi}_k^i)\gamma_{k+1}(\tilde{\xi}_k^{i'})\right)\right]\right]
\end{aligned}
\tag{31}
$$

Proof. Similar to the proof of Proposition 4 in [43].

Proposition A.5. *If $N_{S_k} \geq 2$, and we use fixed assignment splitting at IPS level k then*

$$\mathbb{E}\left\{\overline{\gamma}_{k+1}|\tilde{\xi}_k^1,\ldots,\tilde{\xi}_k^{N_{S_k}}\right\} = \frac{1}{N_{S_k}}\sum_{i=1}^{N_{S_k}}\gamma_{k+1}(\tilde{\xi}_k^i) \tag{32}$$

$$\begin{aligned}&\mathrm{Var}\left\{\overline{\gamma}_{k+1}|\tilde{\xi}_k^1,\ldots,\tilde{\xi}_k^{N_{S_k}}\right\}\\ &= \frac{1}{N_p N_{S_k}}\sum_{i=1}^{N_{S_k}}\left[\gamma_{k+1}(\tilde{\xi}_k^i)\left(1-\gamma_{k+1}(\tilde{\xi}_k^i)\right)\right]\\ &+\frac{\left(N_p \bmod N_{S_k}\right)\left[N_{S_k}-\left(N_p \bmod N_{S_k}\right)\right]}{{N_p}^2 N_{S_k}\left(N_{S_k}-1\right)}\\ &\cdot\left[\sum_{i=1}^{N_{S_k}}\left[\left(\gamma_{k+1}(\tilde{\xi}_k^i)\right)^2\right]-\frac{1}{N_{S_k}}\sum_{i=1}^{N_{S_k}}\sum_{i'=1}^{N_{S_k}}\left[\gamma_{k+1}(\tilde{\xi}_k^i)\gamma_{k+1}(\tilde{\xi}_k^{i'})\right]\right]\end{aligned} \tag{33}$$

Proof. Similar to the proof of Proposition 5 in [43].

Theorem A.2. *Given successful particles $\tilde{\xi}_k^1,\ldots,\tilde{\xi}_k^{N_{S_k}}$ at IPS level k with $N_{S_k} \geq 1$. The dominance of the four splitting methods (MR, MS, RMS, FAS) in terms of* $\mathrm{Var}\left\{\overline{\gamma}_{k+1}|\tilde{\xi}_k^1,\ldots,\tilde{\xi}_k^{N_{S_k}}\right\}$ *is:*

$$\mathrm{V}_{FAS}^k \leq \mathrm{V}_{RMS}^k \leq \mathrm{V}_{MS}^k \leq \mathrm{V}_{MR}^k \tag{34}$$

Proof. Similar to the proof of Theorem 2 in [43].

Theorem A.3. *If IPS levels 1 to k-1 make use of the same type of splitting (either MR, MS, RMS or FAS), then the dominance of the four splitting methods at level k, in terms of* $\mathrm{Var}\left\{\prod_{k'=1}^{k}\overline{\gamma}_{k'}\right\}$ *satisfies:*

$$\mathrm{V}_{FAS\_k} \leq \mathrm{V}_{RMS\_k} \leq \mathrm{V}_{MS\_k} \leq \mathrm{V}_{MR\_k} \tag{35}$$

Proof. Similar to the proof of Theorem 3 in [43].

Theorem A.4. *Under the same type of Splitting (either MR, MS, RMS or FAS) at all levels, then the dominance of the four splitting methods in terms of variance* $\mathrm{V} = \mathrm{Var}\{\overline{\gamma}\}$ *satisfies:*

$$\mathrm{V}_{FAS} \leq \mathrm{V}_{RMS} \leq \mathrm{V}_{MS} \leq \mathrm{V}_{MR} \tag{36}$$

Proof. Similar to the proof of Theorem 4 in [43].

References

[1] J. Hu, J. Lygeros, S.S. Sastry, Towards a theory of stochastic hybrid systems, in: N. Lynch, B.H. Krogh (Eds.), Proc. Hybrid Systems in Computation and Control 2000, in: LNCS number 1790, Springer, 2000, pp. 160–173, 2000.
[2] M.L. Bujorianu, J. Lygeros, Toward a general theory of stochastic hybrid systems, in: H.A.P. Blom, J. Lygeros (Eds.), Stochastic Hybrid Systems, Springer, Berlin, 2006, pp. 3–30.
[3] X. Mao, C. Yuan, Stochastic Differential Equations with Markovian Switching, Imperial College Press, 2006, 2006.
[4] G.G. Yin, C. Zhu, Hybrid Switching Diffusions; Properties and Applications, Springer, 2010, 2010.
[5] K. Kunwai, C. Zhu, On feller and strong feller properties and irreducibility of regime-switching jump diffusion processes with countable regimes, Nonlinear Anal. Hybrid Syst. 38 (2020) 100946, 21 pages.
[6] A.R. Teel, A. Subbaraman, A. Sferlazza, Stability analysis for stochastic hybrid systems: A survey, Automatica 50 (2014) 2435–2456.
[7] J. Lygeros, M. Prandini, Stochastic hybrid systems: a powerful framework for complex, large scale applications, Eur. J. Control 16 (6) (2010) 583–594.
[8] A. Bensoussan, J.L. Menaldi, Stochastic hybrid control, J. Math. Anal. Appl. 249 (2000) 261–288.
[9] X.D. Koutsoukos, Optimal control of stochastic hybrid systems based on locally consistent Markov decision processes, Int. J. Hybrid Syst. (4) (2004) 301–318.
[10] M.K. Ghosh, A. Arapostathis, S.I. Marcus, Optimal control of switching diffusions with application to flexible manufacturing systems, SIAM J. Control Optim. 31 (1993) 1183–1204.
[11] F. Cérou, P. Del Moral, F. Legland, P. Lezaud, Genetic genealogical models in rare event analysis, Lat. Am. J. Probab. Math. Stat. 1 (2006) 181–203.
[12] L.M. Bujorianu, Stochastic Reachability Analysis of Hybrid Systems, Springer, London, 2012.
[13] M. Prandini, J. Hu, Stochastic reachability: Theory and numerical approximation, in: C.G. Cassandras, J. Lygeros (Eds.), Stochastic Hybrid Systems, Taylor & Francis, 2007, pp. 107–137.

[14] A. Abate, M. Prandini, J. Lygeros, S. Sastry, Probabilistic reachability and safety for controlled discrete time stochastic hybrid systems, Automatica 44 (2009) 2724–2734.
[15] A. Lavaei, S. Soudjani, A. Abate, M. Zamani, Automated verication and synthesis of stochastic hybrid systems: A survey, 2021, pp. 1–59, arXiv preprint arXiv:2101.07491.
[16] R. Alur, T. Henzinger, G. Laffierriere, G. Pappas, Discrete abstractions of hybrid systems, Proc. IEEE 88 (2000) 971–984.
[17] A.A. Julius, G.J. Pappas, Approximations of stochastic hybrid systems, IEEE Trans. Automat. Control 54 (2009) 1193–1203.
[18] A Abate, A. D'Innocenzo, M. Di Benedetto, Approximate abstractions of stochastic hybrid systems, IEEE Trans. Autom. Control 56 (2011) 2688–2694.
[19] M.D. Di Benedetto, S. Di Gennaro, A. D'Innocenzo, Hybrid systems and verification by abstraction, in: M. Djemai, M. Defoort (Eds.), Hybrid Dynamical Systems, Springer, 2015, pp. 1–25.
[20] J.A. Bucklew, Introduction to Rare Event Simulation, Springer, New York, 2004.
[21] Z.I. Botev, D.P. Kroese, An efficient algorithm for rare-event probability estimation, combinatorial optimization, and counting, Methodol. Comput. Appl. Probab. 10 (4) (2008) 471–505.
[22] P. L'Ecuyer, F. LeGland, P. Lezaud, B. Tuffin, Splitting techniques, in: B. Tuffin G. Rubino (Ed.), Rare Event Simulation using Monte Carlo Methods, Wiley, 2009, pp. 39–61.
[23] R. Rubinstein, Randomized algorithms with splitting: Why the classic randomization algorithms do not work and how to make them work, Methodol. Comput. Appl. Probab. 12 (2010) 1–50.
[24] J. Morio, M. Balesdent (Eds.), Estimation of Rare Event Probabilities in Complex Aerospace and Other Systems, Woodhead Publishing, 2016.
[25] P. Glasserman, P. Heidelberger, P. Shahabuddin, T. Zajic, Multilevel splitting for estimating rare event probabilities, Oper. Res. 47 (1999) 585–600.
[26] F. Cérou, F. Legland, P. Del Moral, P. Lezaud, Limit theorems for the multilevel splitting algorithm in the simulation of rare events, in: Proc. Winter Simulation Conference. OrlandO, FL, 2005, pp. 682–691.
[27] P. Del Moral, Feynman–Kac Formulae: Genealogical and Interacting Particle Systems with Applications, Springer, 2004.
[28] J. Krystul, F. Le Gland, P. Lezaud, Sampling per mode for rare event simulation in switching diffusions, Stochastic Process. Appl. 122 (7) (2012) 2639–2667.
[29] H.A.P. Blom, J. Krystul, G.J. Bakker, A particle system for safety verification of free flight in air traffic, in: Proc. IEEE Conf. Decision and Control, San Diego, CA, 2006, pp. 1574–1579.
[30] H.A.P. Blom, J. Krystul, G.J. Bakker, Free flight collision risk estimation by sequential MC simulation, in: C.G. Cassandras, J. Lygeros (Eds.), Stochastic Hybrid Systems, Taylor & Francis, 2007a, pp. 249–281.
[31] H.A.P. Blom, G.J. Bakker, J. Krystul, Probabilistic reachability analysis for large scale stochastic hybrid systems, in: Proc. IEEE Conf. on Decision and Control, Vol. 318, 2007b, pp. 2–3189.
[32] H.A.P. Blom, G.J. Bakker, J. Krystul, Rare event estimation for a large scale stochastic hybrid system with air traffic application, in: G. Rubino, B. Tuffin (Eds.), Rare Event Simulation using Monte Carlo Methods, Wiley, 2009, pp. 193–214.
[33] M. Prandini, H.A.P. Blom, G.J. Bakker, Air traffic complexity and the interacting particle system method: An integrated approach for collision risk estimation, in: Proc. American Control Conf., San Francisco, CA, 2011, pp. 2154–2159.
[34] H.A.P Blom, H. Ma, G.J. Bakker, Interacting particle system-based estimation of reach probability for a generalized stochastic hybrid system, IFAC-PapersOnLine 51 (16) (2018) 79–84.
[35] J.P. Hespanha, A model for stochastic hybrid systems with application to communication networks, Nonlinear Anal. 62 (2005) 1353–1383, 2005.
[36] H.A.P. Blom, Stochastic hybrid processes with hybrid jumps, in: Proc. IFAC Conf. Analysis and Design of Hybrid Systems, Saint-Malo, Brittany, France, 2003, 16-18 2003.
[37] M.K. Ghosh, A. Bagchi, Modeling stochastic hybrid systems, in: J. Cagnol, J.P. Zolèsio (Eds.), System Modeling and Optimization. Proc. 21st IFIP TC7 Conference, Sophia Antipolis, France, July 2004, 2004, pp. 269–279.
[38] F. Xi, G. Yin, C. Zhu, Regime-switching jump diffusions with non-lipschit coefficients and countably many switching states: existence and uniqueness, feller, and strong feller properties, in: G. Yin, Q. Zhang (Eds.), Modeling, Stochastic Control, Optimization and Applications, Springer, 2019, pp. 571–599.
[39] J. Krystul, A. Bagchi, H.A.P. Blom, On Strong Markov Property of Solutions To Stochastic Differential Equations on Hybrid State Spaces, Report 28th 2011, U. of Twente, 2011, https://repository.tudelft.nl/islandora/object/uuid%3A948fc4dd-66f5-42bc-82e6-8770d371add3.
[40] H.A.P. Blom, Feller property of regime-switching jump diffusion processes with hybrid jumps, in: Stochastic Analysis and Applications, 2022, Forthcoming.
[41] J. Krystul, Modelling of Stochastic Hybrid Systems with Applications to Accident Risk Assessment (Ph.D. thesis), University of Twente, The Netherlands, 2006, 2006.
[42] J. Krystul, H.A.P. Blom, A. Bagchi, Stochastic differential equations on hybrid state spaces, in: C.G. Cassandras, J. Lygeros (Eds.), Stochastic Hybrid Systems: Recent Developments and Research Trends, Taylor & Francis/CRC Press, 2007, pp. 15–45, 2007.
[43] H. Ma, H.A.P. Blom, Fixed assignment vs. random assignment in multilevel importance splitting for estimating stochastic reach probability, Methodol. Comput. Appl. Probab. (2021) Accepted 17th 2021.
[44] M. Hutzenthaler, A. Jentzen, P.E. Kloeden, Strong and weak divergence in finite time of Euler's method for stochastic differential equations with non-globally Lipschitz continuous coefficients, in: Proc. R. Soc. a., Vol. 467, 2011, pp. 1563–1576.
[45] P. Glasserman, Monte Carlo Methods in Financial Engineering, Springer Science & Business Media, 2004.